http://dx.doi.org/10.6113/TKPE.2016.21.3.238

자동 지령모드절환 기능을 갖춘 PMSG MV 해상 풍력 발전기의 직접전력제어 방법

권국민[1], 서용석†

Automatic Command Mode Transition Strategy of Direct Power Control for PMSG MV Offshore Wind Turbines

Gookmin Kwon[1] and Yongsug Suh†

Abstract

In this study, an automatic command mode transition strategy of direct power control (DPC) is proposed for permanent magnet synchronous generators (PMSGs) medium-voltage (MV) offshore wind turbines (WTs). Benchmarking against the control methods are performed based on a three-level neutral-point-clamped (NPC) back-to-back type voltage source converter (VSC). The ramping rate criterion of complex power is utilized to select the switching vector in DPC for a three-level NPC converter. With a grid command and an MPPT mode transition strategy, the proposed control method automatically controls the generated output power to satisfy a grid requirement from the hierarchical wind farm controller. The automatic command mode transition strategy of DPC is confirmed through PLECS simulations based on Matlab. The simulation result of the automatic mode transition strategy shows that the proposed control method of VOC and DPC achieves a much shorter transient time of generated output power than the conventional control methods of MPPT and VOC under a step response. The proposed control method helps provide a good dynamic performance for PMSGs MV offshore WTs, thereby generating high quality output power.

Key words: Direct power control, Dynamic response, Mode transition, Maximum power point tracking, Wind power system

1. Introduction

Recently, wind power system is one of the fastest growing renewable energy systems. In the multi-MW wind turbine market, the maximum power rating of a commercial wind turbine has been increased more than 5 MW with a view to generate more power from wind power sites[1]. Continually wind power installation has been increasing both in number and size of individual wind turbine unit. In large scaled MW-range wind turbines, PMSG type wind turbine involving a full-scale power converter becomes a trend due to its superb performance in active and reactive power generation[2]. Power electronic converters in medium-voltage level are generally realized as Multi-level (ML) Voltage Source Converters (VSC) instead of two-level VSCs in order to improve the performance factors regarding switch power losses, harmonic distortion, and common mode voltage/current[3]. In the family of multilevel inverters, the three-level topology, called Neutral Point Clamped (NPC) inverter, is one of the few topologies that have received a reasonable consensus in the high power community[4]. These NPC inverters have also been implemented successfully in the industrial applications

Paper number: TKPE-2016-21-3-7
Print ISSN: 1229-2214 Online ISSN: 2288-6281
† Corresponding author: ysuh@jbnu.ac.kr, Dept. of Electrical Engineering, Smart Grid Research Center, Chonbuk Nat'l University
Tel: +82-63-270-3381 Fax: +82-63-270-3381
[1] Dept. of Electrical Engineering, Smart Grid Research Center, Chonbuk Nat'l University
Manuscript received Mar. 8, 2016; revised Mar. 31, 2016; accepted Apr. 20, 2016

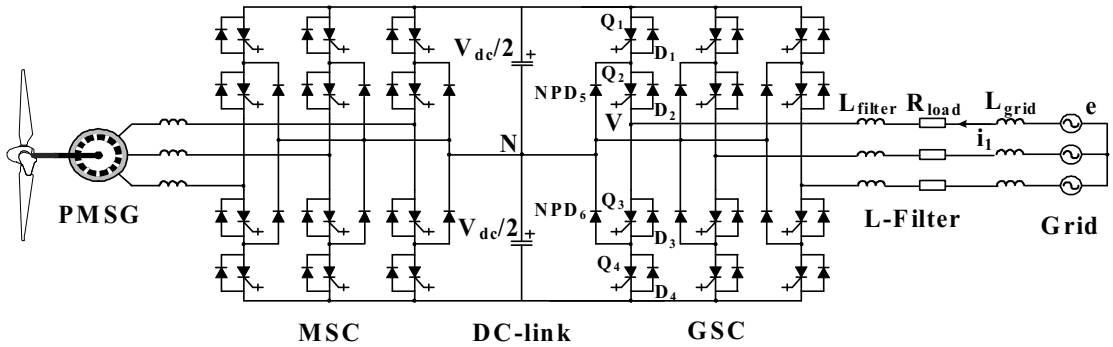

Fig. 1. Three-level neutral-point-clamped (3L-NPC) back-to-back configuration for PMSG MV wind turbines.

for high power drives and wind turbines[5]. As the penetration of renewable resources into the grid is rapidly increasing, high-performance control of power converters is a must to maintain high power quality and system stability. In particular, large-scaled offshore wind farms have become a subject to various grid codes demanding tougher grid adaptive features such as LVRT, voltage support, frequency stability, ramp rate control, rapid shut down control, and etc[6]. To satisfy these requirements, fast and accurate active/reactive power regulation is essential[7]. In wind power systems, most of previous studies regarding power control scheme have focused on the Maximum Power Point Tracking (MPPT) with optimal tip speed ratio and optimal torque control of the machine-side converter irrespective of the type of generator used[8]. Based on the principle of Direct Torque Control (DTC) strategy for ac machines[9],[10], alternative control approach, namely Direct Power Control (DPC) was developed for the control of three-phase grid-connected two-level VSC[11],[12]. This DPC method is designed to effectively obtain the requested amount of power and improve the steady-state and transient performance, and also maintain the simplicity and robustness of the control system. Considering various grid codes and active and reactive power generation requirements imposed on large-scaled offshore wind farms, the efficient utilization of DPC method together with MPPT control and mode transition strategy for wind turbines has not been explored in detail in previous literatures. In particular, seamless transition between grid command and MPPT mode with a DPC method did not get enough attention in prior arts considering its growing importance in the practical wind farm control system.

This paper addresses an automatic command mode transition strategy of DPC method applied for the full-scaled power converter in PMSG wind turbines. Entire control scheme for both of machine-side converter (MSC) and grid-side converter (GSC) employing DPC is introduced. In addition, this paper proposes a novel way of securing seamless transition between grid command mode and MPPT mode under the sudden change of reference power command. In this paper, automatic command mode transition strategy of DPC method has been adopted in controlling the GSC of a wind turbine. Also ramping rate criterion based on complex power is utilized to select a proper switching vector in a three-level NPC converter. Control of MSC employs a dc-link voltage regulation strategy, i.e. Voltage Oriented Control (VOC) using a PI controller. The control mode transition strategy between grid command mode and MPPT is structured by sensing a dc-link voltage error with hysteresis band. This mode changer is triggered by either grid command from the wind farm controller or external interruption such as wind speed variation and grid disturbances. Therefore, the proposed control method of VOC and DPC makes it easier to comply with various grid codes and requirements on wind farms.

This paper is structured as follows. In Sections 2, basic modeling for direct power control is described in three-level NPC converter. In Section 3, conventional control scheme and proposed control scheme are presented and compared. The simulations results comparing conventional and proposed control scheme are explained in Section 4. Finally, conclusion is given in Section 5.

2. Direct Power Control (DPC) Modeling for Three-level NPC Converter

For a typical wind turbine of PMSG type, the GSC

of a three-level rectifier is shown in Fig. 1[11],[12]. DPC of GSC is implemented based on the rectifier model in a stationary $\alpha\beta$-frame. e and i_1 are space vector of grid voltage and current in Fig. 1. V is space vector of rectifier voltage at the pole side of GSC. L_{filter} and L_{grid} are filter inductance and grid inductance. R_{load} is load resistance designating the series equivalent resistance value at the ac side of GSC. The complex power at the grid side can be represented as

$$S=\frac{3}{2}(ei_1^*)=\frac{3}{2}(|e|e^{j\omega t}i_1^*) \tag{1}$$

Differentiating complex power of (1) is given as in (2)

$$\frac{dS}{dt}=j\omega S+\frac{1.5}{L_{filter+grid}}(|e|^2-eV^*-R_{load}ei_1^*) \tag{2}$$

According to (2), differentiating complex power can be further developed as

$$\frac{dS}{dt}=j\omega S+\frac{1.5}{L_{filter+grid}}(|e|^2-eV^*)-\frac{R_{load}S}{L_{filter+grid}} \tag{3}$$

V is represented as $V_n e^{j\theta_n}$ where V_n and θ_n depend on the switching state of GSC, i.e. large, middle, and small vectors as shown in Fig. 2. Derivative term of complex power of (3) can be divided into real and imaginary component. In the case of switching states of large vector, the real and imaginary terms become as the following.

$$\begin{aligned}\frac{dP}{dt}&=1.5\left(\frac{|e|^2-|V_n||e|\cos(\omega t-\theta_n)}{L_{filter+grid}}\right)-\frac{R_{load}}{L_{filter+grid}}P-\omega Q\\ \frac{dQ}{dt}&=1.5\left(\frac{-|V_n||e|\sin(\omega t-\theta_n)}{L_{filter+grid}}\right)-\frac{R_{load}}{L_{filter+grid}}Q+\omega P\end{aligned} \tag{4}$$

Based on (4), ramping rate of instantaneous active and reactive power can be computed under various operating conditions.

The main task of DPC employed in this paper is to regulate both the active and reactive power exchanged with the ac grid. The controller is to choose the proper switching state of GSC in order to regulate the measured variables of active and reactive power output within the target range. Therefore, the model of ramping rate of instantaneous active and reactive power plays a critical role in DPC method. This model of ramping rate eventually implement a

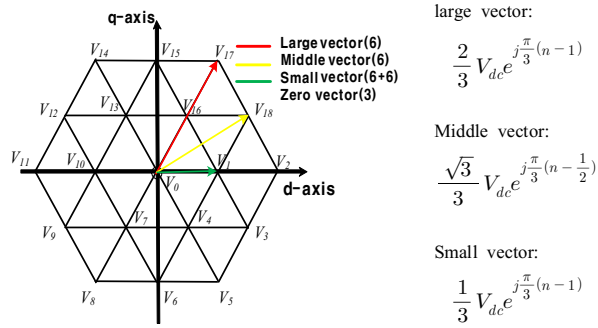

Fig. 2. 3-level vector diagram (large, middle, and small vectors).

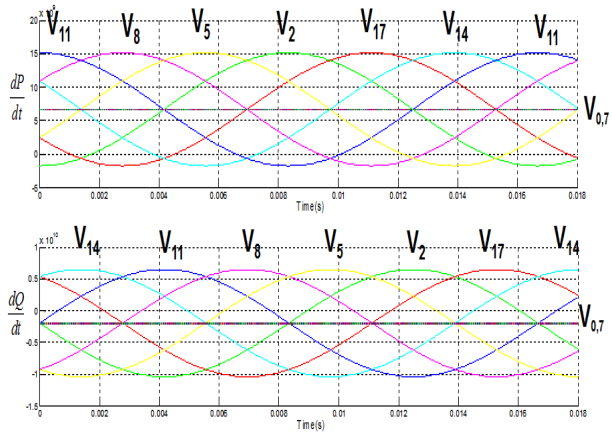

Fig. 3. Ramping rate of instantaneous active and reactive power by using large vectors in 12 different sectors. (P=5 MW, Q=0 MVAr).

switching vector selection criteria and table for GSC. Plugging relevant parameter values of the particular example case considered in this paper into (4) yields a sinusoidal waveform with non-zero offset. Under the conditions of large vectors, ramping rate of instantaneous active and reactive power of (4) are obtained and illustrated in Fig. 3. Following the same approach as in large vectors, the ramping rate of instantaneous active and reactive power for the cases of middle and small vectors can be similarly obtained.

The selection of switching vector is done in such a way that the active and reactive output power are kept within the target hysteresis band. Therefore, it is important to correlate each switching vector with the sign of ramping rate of active and reactive power, i. e. increasing or decreasing active and reactive output power. In principle, there are four possible sign combinations with respect to ramping rate of active and reactive power such as $\frac{dP}{dt}(+)/\frac{dQ}{dt}(+)$, $\frac{dP}{dt}(+)/\frac{dQ}{dt}(-)$, $\frac{dP}{dt}(-)/\frac{dQ}{dt}(+)$, $\frac{dP}{dt}(-)/\frac{dQ}{dt}(-)$. Corresponding to one of these four sign combinations of ramping rate, there

TABLE I
SWITCHING VECTOR TABLE FOR DPC USING RAMPING RATE CRITERION OF COMPLEX POWER

Rate condition	0~ 30°	30~ 60°	60~ 90°	90~ 120°	120~ 150°	150~ 180°	180~ 210°	210~ 240°	240~ 270°	270~ 300°	300~ 330°	330~ 360°
dP/dt(+), dQ/dt(+)	V_{13}	V_{12}	V_{10}	V_9	V_7	V_6	V_4	V_3	V_1	V_{18}	V_{16}	V_{15}
dP/dt(+), dQ/dt(-)	V_4	V_4	V_1	V_1	V_{16}	V_{16}	V_{13}	V_{13}	V_{10}	V_{10}	V_7	V_7
dP/dt(-), dQ/dt(+)	V_{18}	V_{17}	V_{15}	V_{14}	V_{12}	V_{11}	V_9	V_8	V_6	V_5	V_3	V_2
dP/dt(-), dQ/dt(-)	V_2	V_{18}	V_{17}	V_{15}	V_{14}	V_{12}	V_{11}	V_9	V_8	V_6	V_5	V_3

are particular switching vectors assigned depending on the angle position. These switching vectors can be found out from the graphs of ramping rate of instantaneous active and reactive power as given in Fig. 3. In Table I, switching vectors which has the maximum value for ramping rate function of complex power[13]. This selection criteria is intended to compromise between ramping rate of active and reactive power so that both active and reactive power are well regulated within the target hysteresis band at the same time by the chosen switching vector. The final selected switching vectors satisfying these selection guidelines for each angle position from 0-30° to 330-360° are summarized in Table I.

3. Conventional and Proposed Control Scheme for Entire System

3.1 Conventional control scheme

Wind energy has an intrinsic intermittent physical properties as wind speed changes throughout the day. In general, the amount of power output from a wind energy conversion system depends upon the accuracy with which the peak power points are tracked by MPPT controller of the MSC control system irrespective of the type of generator as illustrated in Fig. 4[8]. Among many MPPT approaches reported, speed control method based on optimal tip speed ratio and torque control based on squared rotor speed are widely used in wind industry[14]. MPPT equation is expressed as

$$P_m = \frac{1}{2}\pi\rho C_p(\lambda,\beta)R^2 v_{wind}^3 \quad (5)$$

$$\omega_m^* = \frac{\lambda_{opt} v_{wind}}{R} \quad (6)$$

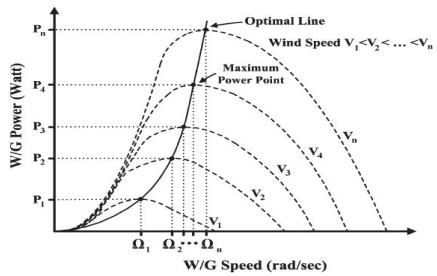

Fig. 4. Maximum power point tracking (MPPT) curve at various wind speeds.

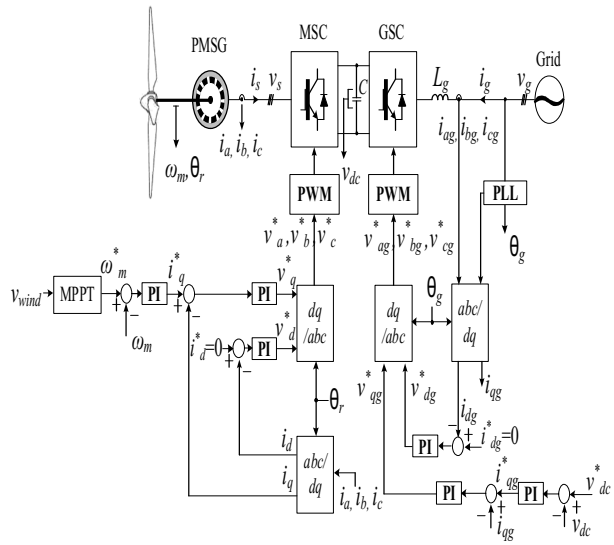

Fig. 5. Control block diagram of conventional control of MPPT with optimal tip speed ratio and VOC for PMSG MV wind turbines.

$$T_m^* = k_{opt}\omega_m^2 \quad (7)$$

Utilizing (5) and (6), the conventional control block diagram of MPPT with optimal tip speed ratio and Voltage Oriented Control (VOC) is described in Fig. 5. Also the conventional control block diagram of MPPT with optimal torque control and VOC using (5) and (7) is presented in Fig. 6.

The control strategys of GSC is to simply transfer generated active power from MSC to ac grid. It means that GSC regulates a dc-link voltage using a PI controller. This VOC method has advantages of fixed switching frequency and less sensitivity to line inductance variation. But coordinate transformation and decoupling between active and reactive components are required[15]. In modern offshore wind farms of large scale, as the penetration of renewable resources into the grid is rapidly increasing, high performance control of power converters is a must to maintain high power quality and system stability.

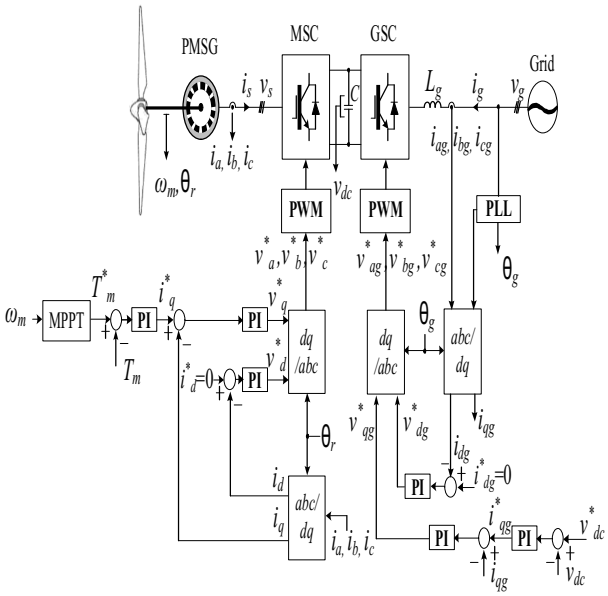

Fig. 6. Control block diagram of conventional control of MPPT with torque reference proportional to speed squared and VOC for PMSG MV wind turbines.

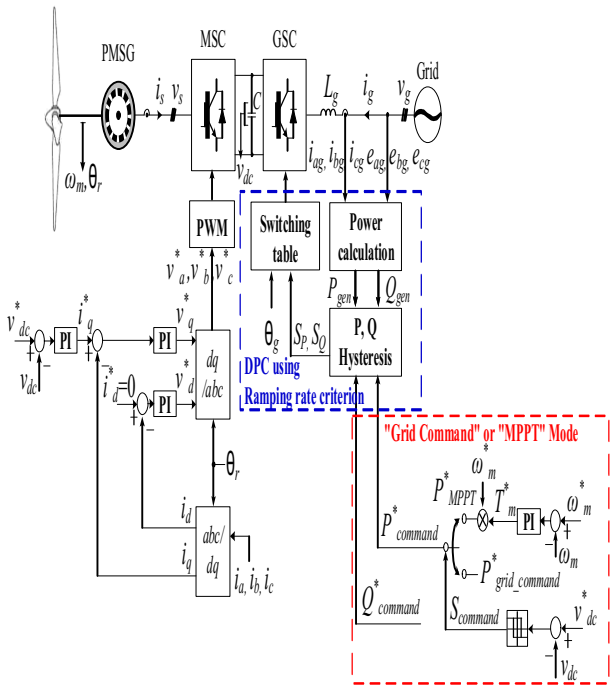

Fig. 7. Proposed control of VOC and DPC block diagram for PMSG MV wind turbines.

Increasing penetration of large wind farms generally requires that the wind farms behave in a similar dynamic behavior as the conventional thermal power plants with a view to maintain the reliable grid control. Therefore, instead of MPPT with optimal tip speed ratio and torque control strategys, which are typically designed to extract the maximum amount of generated wind power from an economical point of view, the control strategys realizing accurate and prompt generation of active and reactive power following the command from the grid operator is more compatible with the reinforcing grid codes. The conventional control schemes of MPPT and VOC described in Fig. 5 and 6 has become less optimized to satisfy various grid requirements imposed on the PMSG MV offshore wind farms.

3.2 Proposed control scheme

In general, MPPT and VOC control methods does not have a good dynamic performance under varying active power command. There has been a growing demand of grid adaptive features on large scaled offshore wind farms. These features involve transient and rapid variation of active and reactive power output from wind farms in the comparable level as conventional thermal power plants. In general, DPC does not require a separate Pulse-Width Modulation (PWM) voltage block, current regulation loop, and rotating transformation. Therefore it has a good dynamic performance and robustness independent of the accuracy of PLL block[15],[16]. The proposed control scheme of VOC and DPC in this paper is presented in Fig. 7.

The proposed control strategy is made up of two controller, DPC for GSC and *dq*-current regulator for MSC with dc-link voltage regulation feature. DPC for GSC acts on a reference power command while dc-link voltage regulator of MSC simply provides the demanded power from GSC. This feature of the proposed control strategy with respect to the role sharing between GSC and MSC in determining power generation is almost opposite to that of conventional control strategy in Fig. 5 and 6. The reference power command to DPC in GSC control block may come from two different sources; grid command from a wind farm controller (*grid command mode*) and the MPPT block of individual wind turbine controller (*MPPT mode*). The transition of this power command source, which is referred to as *Control Mode Change* in this paper, depends on the available wind speed and hysteresis error of dc-link voltage regulator. In principle, the wind turbine cannot always meet the power generation command from wind farm controller when the available wind speed is less than the power demand. Under this particular condition, the controller of individual wind turbine is designed to opt

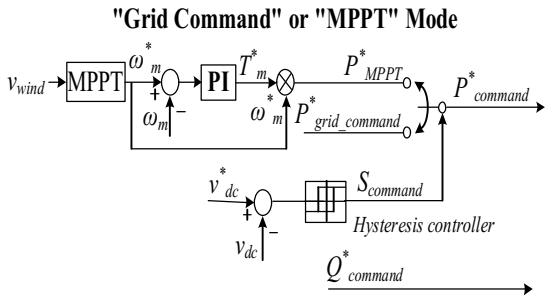

Fig. 8. Grid command or MPPT mode change block diagram.

out of grid command mode and enter into MPPT mode. This mode change is triggered by the error signal from dc-link voltage regulator as illustrated in Fig. 8. This transition feature based on the dc-link voltage error provides a smooth and seamless mode changing between grid command mode and MPPT mode. As long as there is enough wind resources, the individual wind turbine can cope with the reference power command from the wind farm controller under grid command mode. Unlike the reference command for the active power generation, the reference command for the reactive power generation in GSC is not subject to different control modes. Instead, the reactive power generation is only limited by the total available peak current capability of GSC and the size of active power generation at a certain operating point.

As a result, the proposed control scheme has two novel features as compared to the prior arts. The first feature is that the automatic command mode changing method is complemented by dc-link error signal in addition to already existing external command mode changer. The second feature is that the systematic integration of this automatic command mode changing method into the overall structure of VOC and DPC in this paper.

4. Simulation Verification

The simulation is performed based on the parameters of 5 MW PMSG MV back-to-back type voltage source converter as specified in Table Ⅱ[17],[18]. Since the converter is a 3L-NPC type connected to the ac line of 4160 V, the nominal dc-link voltage is chosen to be 7 kV. The PWM carrier frequency adopted for the MSC of VOC is set to 1020 Hz. Average switching frequency of GSC in the proposed

TABLE Ⅱ
SIMULATION PARAMETERS OF 5 MW PMSG WIND TURBINE SYSTEM

Parameter	Symbol	Value	Per unit
Output power	$P_{rated-out}$	5 MW	1.0
Rated wind speed	V_{wind}	12 m/s	-
Machine side input voltage	V_{ll_MSC}	4.16 kV	1.0
Machine side input current	$I_{MSC-input}$	708 A	1.0
PWM carrier frequency	$f_{MSC-PWM}$	1020 Hz	-
DC-link voltage	$V_{DC-link}$	7 kV	-
DC-link capacitance	$C_{DC-link}$	3 mF	-
Grid frequency	f_{grid}	60 Hz	1.0
Grid side input voltage	V_{ll_GSC}	4.16 kV	1.0
Grid side input current	$I_{GSC-input}$	708 A	1.0
Sampling frequency	f_{DPC_samp}	40 kHz	-
Grid side inductance	L_{grid}	1.56 mH	0.17
AC filter inductance	L_{filter}	1.5 mH	0.16
Load resistance	R_{load}	0.35 mΩ	0.013

control method is set to 480 Hz. In order to effectively confirm the proposed control strategy, the simulation is performed under three different operating conditions; Case 1: steady-state condition of power generation of 5 MW (MPPT mode), Case 2: control mode change (MPPT mode → grid command mode), and Case 3: control mode change (MPPT mode → grid command mode → MPPT mode). Additionally, the proposed control scheme is compared with both conventional control strategies of MPPT.

4.1 Case 1: steady-state condition of power generation of 5 MW (MPPT mode)

Under Case 1, the converter is controlled to generate the active power of 5 MW and the reactive power of 0.35 MVar resulting in the power factor of 0.998 leading. The waveforms generated by the proposed control method under the steady-state condition are described in Fig. 9-11. In Fig. 9, a set of dc-link voltage waveform are illustrated. Switching signal and its waveforms for grid adaptive DPC in GSC are obtained and shown in Fig. 10. Fig. 11 shows the instantaneous active and reactive output power waveform.

In Fig. 11, the instantaneous active and reactive output power waveform have a relatively large steady-state ripple as compared to the conventional

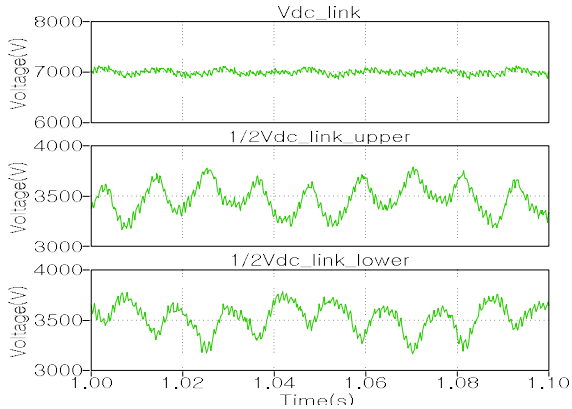

Fig. 9. DC-link voltage waveform under steady-state condition.

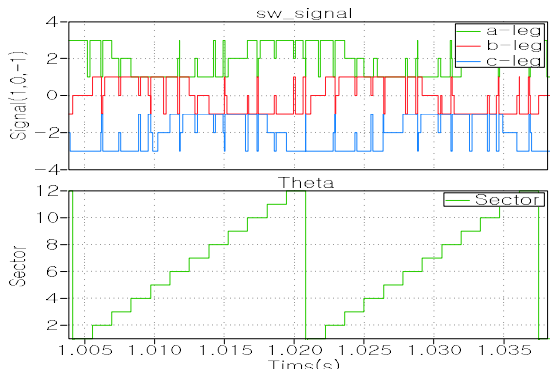

Fig. 10. Switching signals and sectors for DPC in GSC waveform under steady-state condition.

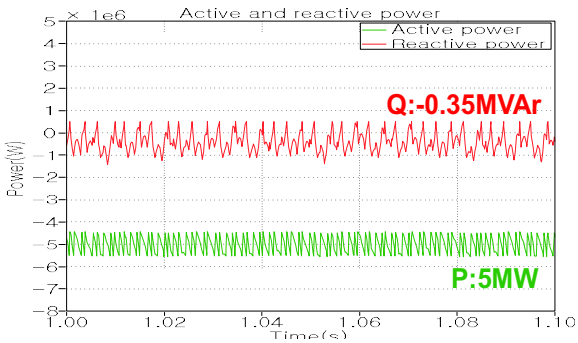

Fig. 11. Active and reactive output power waveform under steady-state condition.

methods. This large power ripple attributes to the fact that some of switching vectors have unwanted sign reversals of dP/dt and dQ/dt. This critical characteristic eventually results in large THD of grid side current. Recently, there have been several methods introduced in the literatures such as duty control or cost-function to solve this problem[11],[12].

4.2 Case 2: control mode change (MPPT mode → grid command mode)

Under Case 2, the transient behavior of proposed control method of VOC and DPC is simulated according to the scenario described in Table Ⅲ. Initially the control mode is set to MPPT mode of generating the rated output power of 5 MW under the rated wind speed of 12 m/s. Then, at the simulation time of 1.0 sec, the control mode is deliberately changed from MPPT mode to grid command mode by shifting the reference power command from MPPT block to the wind farm controller. The new reference power command from the grid is set to 4.5 MW under the same wind speed of 12 m/s.

TABLE Ⅲ
CASE 2, SIMULATION CONDITION OF CONTROL MODE CHANGE (FROM MPPT TO GRID COMMAND MODE)

Target / Time	~ 1s	1s ~ 2.5s
Reference power (Fixed wind speed: 12m/s)	Active power: 5MW (Rated power:5MW)	Active power: 4.5MW (Rated power:5MW)
Mode	MPPT	Grid command
Condition	Steady-state	Decreased active power reference

In order to confirm the superior behavior of the proposed control method of VOC and DPC, the major operating waveforms are compared to those of conventional control scheme under the same operating scenario. The simulation waveforms corresponding to conventional control of MPPT with optimal tip speed ratio and VOC method are given in Fig. 12-15. The corresponding simulation waveforms for proposed control of VOC and DPC method are also shown in Fig. 16-19. The waveforms of instantaneous active and reactive power for conventional and proposed control method are presented in Fig. 12 and 16, respectively. It is evident from Fig. 12 and 16 that the proposed control method of VOC and DPC exhibits better transient behavior with less overshoot and shorter settling time as compared to the conventional method of MPPT wit optimal tip speed ratio and VOC. This is because the GSC of the proposed control method of VOC and DPC reacts promptly to the change of power command and the MSC provides the just enough amount of power to keep the dc-link voltage within the regulation band. Therefore, the MSC can avoid the severe transient overshoot due to relatively low control bandwidth of speed regulation loop. However, in conventional control method of MPPT with optimal tip speed ratio and VOC, the power command is translated into the speed command for MSC. Thus, the abrupt change of

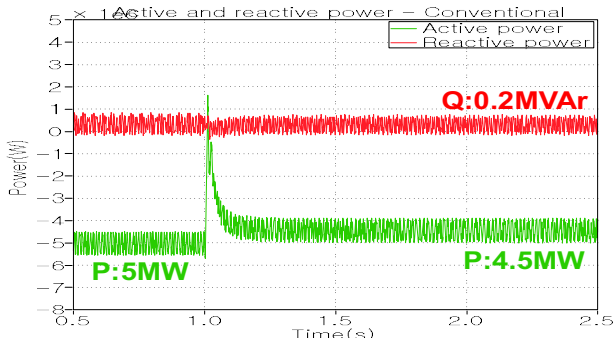

Fig. 12. Active and reactive power of conventional control method.

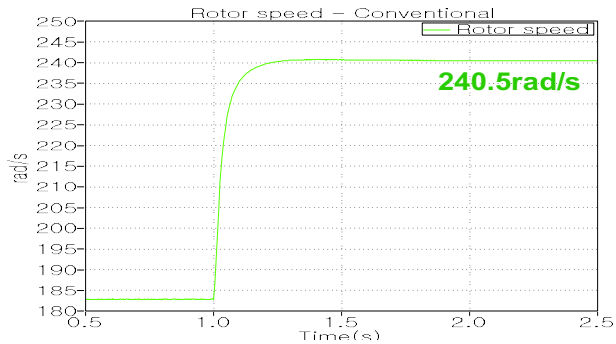

Fig. 13. Rotor speed of conventional control method.

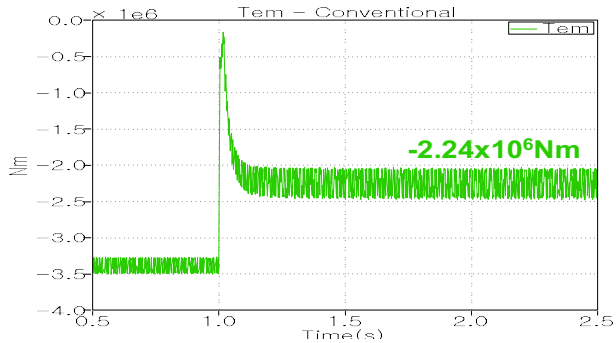

Fig. 14. Electromagnetic torque of conventional control method.

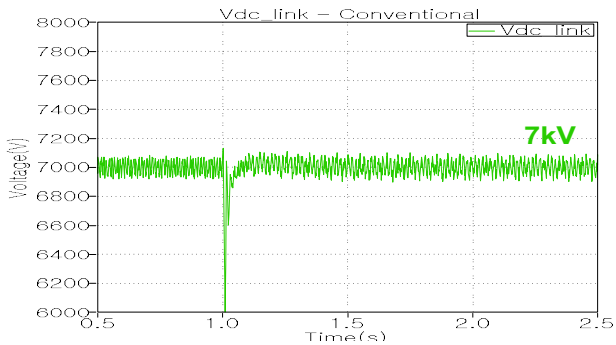

Fig. 15. DC-link voltage of conventional control method.

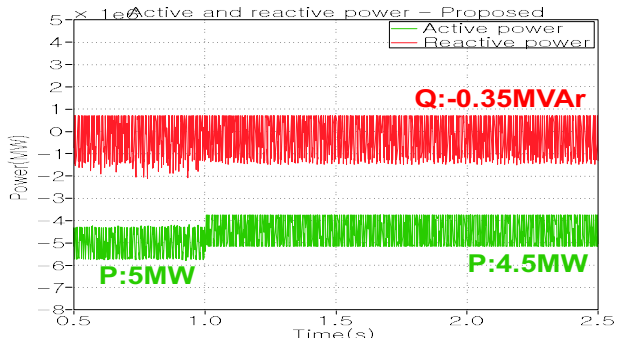

Fig. 16. Active and reactive power of proposed control method.

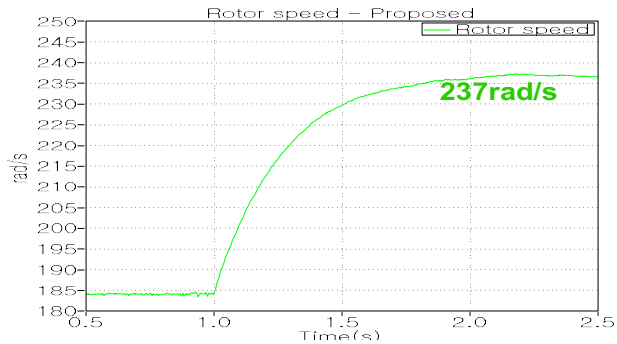

Fig. 17. Rotor speed of proposed control method.

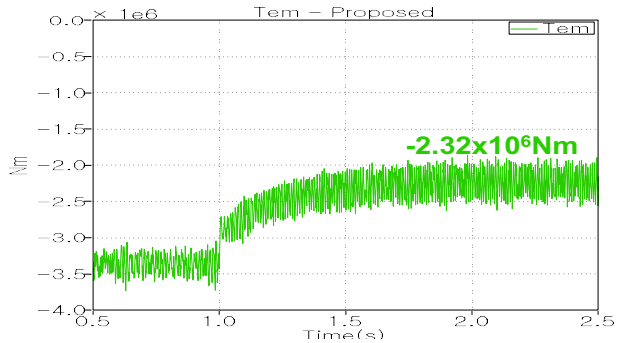

Fig. 18. Electromagnetic torque of proposed control method.

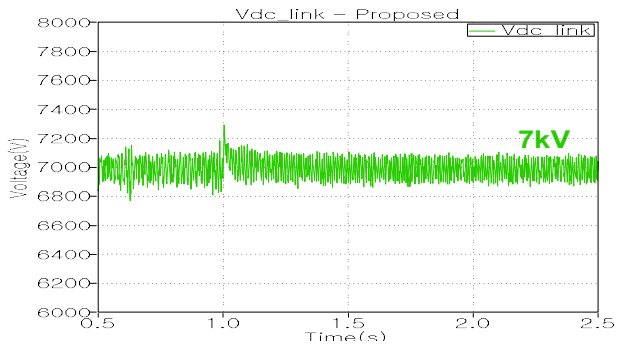

Fig. 19. DC-link voltage of proposed control method.

power command results in the similar step-wise change of speed command. This step-wise change of speed command causes the large torque and dc-link voltage undershoot in the conventional control of MPPT with optimal tip speed ratio and VOC method as depicted in Fig. 14 and 15, respectively. This problems can be mitigated by adding some ramping rate on the speed command or employing different MPPT strategies such as torque control based on squared rotor speed. The comparison result against this MPPT method using torque control under Case 2 is explained in Section 4.4.

TABLE Ⅳ
CASE 3, SIMULATION CONDITION OF CONTROL MODE CHANGE (FROM MPPT TO GRID COMMAND MODE AND FROM GRID COMMAND TO MPPT MODE)

Target / Time	~ 1s	1s ~ 1.21s	1.21s ~ 2.5s
Reference power (Fixed wind speed: 11.2m/s)	Active power: 4.5MW (Rated power:5MW)	Active power: 5MW (Rated power:5MW)	Active power: 4.5MW (Rated power:5MW)
Mode	MPPT	Grid command	MPPT
Condition	Steady-state	Increased active power reference	Steady-state
Minimum V_{dc_link}	V_{dc_link} =0.9pu → 6.3 kV (Rated V_{dc_link} =7 kV)		

4.3 Case 3: control mode change (MPPT mode → grid command mode → MPPT mode)

Under Case 3, the performance of control mode changing method as shown in Fig. 8 is evaluated. The controller is subject to two mode changing transients as explained in Table Ⅳ. Initially the control mode is set to MPPT mode of 4.5 MW. The wind speed is assumed to be constant at 11.2 m/s throughout this simulation case. At the simulation time of 1.0 sec, the control mode is changed purposely to grid command mode with the new reference power input of 5 MW from the wind farm controller. This scenario is to model the possible increase of power command by a grid operator to comply with the grid code. Then, since the available wind speed is not enough for the wind turbine to continuously generate the command power of 5 MW, the stored energy both in the inertia of rotor and dc-link capacitor is dissipated resulting in the drop of speed and dc-link voltage. At the moment when the dc-link voltage decreases below the minimum hysteresis error band, i.e. 10% of rated value, the control mode is automatically set back to MPPT mode again to continuously generate the available active power of 4.5 MW. This automatic mode changing takes place at the simulation time of 1.21 s approximately.

The key waveforms of proposed controller under Case 3 are illustrated in Fig. 20-23. Using a command mode changer, characteristics of proposed control method of VOC and DPC provide a good dynamic performance and improve a transient conditions for PMSG MV offshore wind turbine in order to generate a high quality output power.

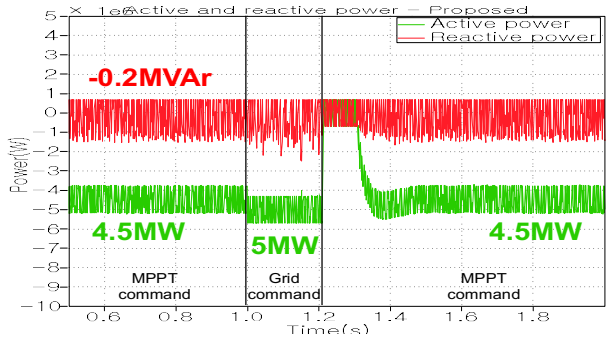

Fig. 20. Active and reactive power of changed command mode.

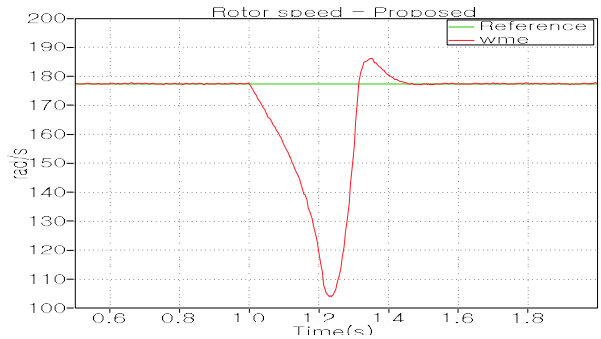

Fig. 21. Rotor speed of changed command mode.

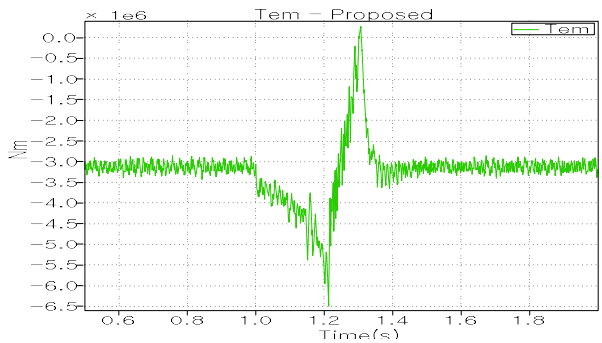

Fig. 22. Electromagnetic torque of changed command mode.

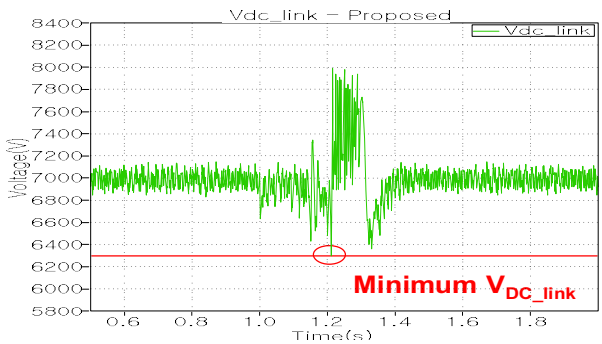

Fig. 23. DC-link voltage of changed command mode.

4.4 Comparison of conventional control method of MPPT based on torque control

This section is to provide the comparison result of other benchmarking conventional MPPT method; MPPT with optimal torque control in Fig. 6. The

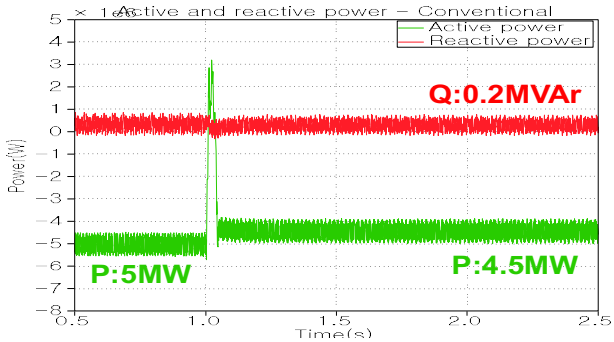

Fig. 24. Active and reactive power from conventional control method of MPPT with optimal torque control.

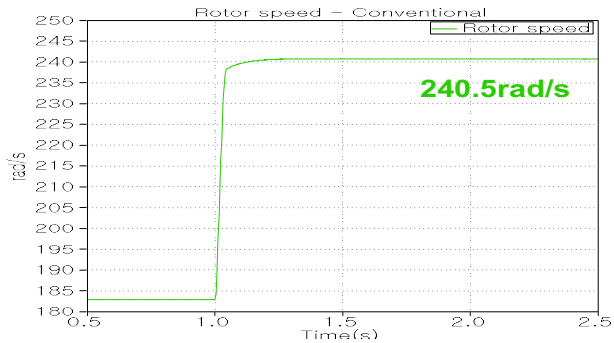

Fig. 25. Rotor speed from conventional control method of MPPT with optimal torque control.

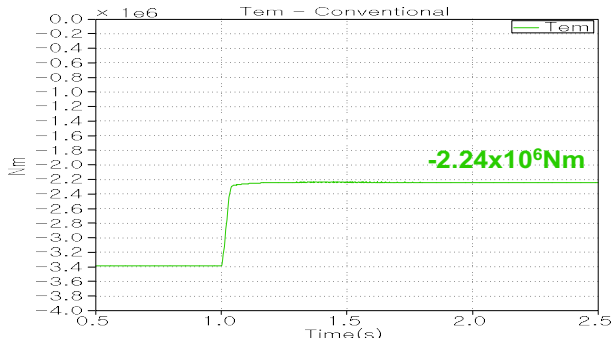

Fig. 26. Electromagnetic torque from conventional control method of MPPT with optimal torque control.

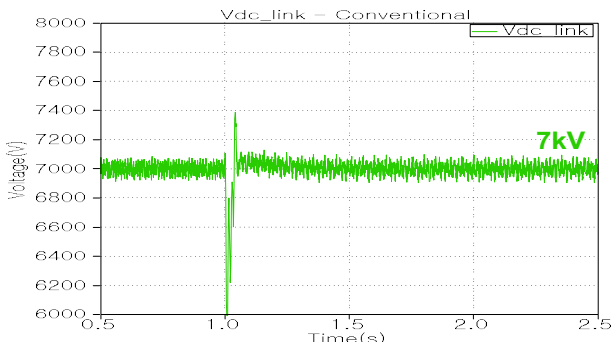

Fig. 27. DC-link voltage from conventional control method of MPPT with optimal torque control.

waveforms generated by the conventional control method of MPPT with optimal torque control under the same step-response condition of Case 2 are described in Fig. 24-27. According to these simulation results of MPPT with optimal torque control, the transient response of the electromagnetic torque is improved showing a much shorter transient time than that of conventional control scheme of MPPT with optimal tip speed ratio as illustrated in Fig 14 and 26, respectively. However, even though the torque response is improved, the response of instantaneous active power is still inferior to that of the proposed control method as shown in Fig. 16 and 24. As mentioned in Section 3.2, the proposed control method of VOC and DPC is suitable to solve the above problem and satisfy a grid requirement.

5. Conclusion

This paper propose an automatic command mode transition strategy of direct power control for PMSGs MV offshore wind turbines. The proposed control method involves a dc-link voltage regulation for a MSC and direct power control for a GSC using an automatically convertible command mode controller. In addition, the ramping rate criterion based on the complex power is used to select the proper switching vector in DPC controller. It is shown that the active and reactive power can be directly controlled under various grid fault conditions and requirements of automatic generation control in a wind farm level. In the transient condition of power reference variation, due to DPC characteristic, proposed control method of VOC and DPC achieves a much shorter transient time in the step response of output power as compared to the conventional control methods of MPPT and VOC. The proposed control method of VOC and DPC makes it possible to provide a good dynamic performance for PMSGs MV offshore wind turbines in order to generate a high quality output power under grid fault or steady-state condition.

References

[1] BTM Consult ApS: World Market Update 2008, Forecast 2009-2013.

[2] F. toque, W. Xie, Z. Li, and Y. Zhang, "Power electronics converters for wind turbine systems," *IEEE Trans. on Industry Applications*, Vol. 48, No. 2, pp. 708-719, Mar./Apr. 2012.

[3] B. Wu, High-Power Converters and AC Drives, Piscataway, NJ, *IEEE Press*, 2006, ISBN 978-0-471-731-9.

[4] A. Nabae, I. Takahashi, and H. Akagi, "A new neutral point clamped PWM inverter," *IEEE Trans. on Industry*

Applications, Vol. IA - 17, No. 5, pp. 518-523, Sep. 1981.
[5] Information about ACS1000 medium voltage drive product at http://www.abb.com/motor& drives.
[6] T. H. Nguyen, D. Lee, "Ride-through technique for PMSG wind turbines using energy storage system," *Journal of Power Electronics*, Vol. 10, No. 6, pp. 733 - 738, Nov. 2010.
[7] Y. Zhang, M. Liserre, R. Teodorescu, and P. Rodriguez, "Low complexity model predictive power control : Double vector based approach," *IEEE Trans. on Industrial Electronics*, Vol. 61, No. 11, pp. 5871 - 5880, Nov. 2014.
[8] E. Koutroulis, K. Kalaitzakis, "Design of a maximum power tracking system for wind energy conversion applications," *IEEE Trans. on Industrial Electronics*, Vol. 53, No. 2, pp. 486 - 494, Apr. 2006.
[9] I. Takahashi and T. Noguchi, "A new quick response and high-efficiency control strategy of an induction motor," *IEEE Trans. on Industry Applications*, Vol. 22, No. 5, pp. 820 - 827, Aug. 1986.
[10] M. Depenbrock, "Direct self-control (DSC) of inverter-fed induction machine," *IEEE Trans. on Power Electronics*, Vol. 3, No. 4, pp. 420 - 429, Jul. 1988.
[11] Y. Zhang, Z. Li, Y. Zhang, W. Xie, Z. Piao, and C. Hu "Performance improvement of direct power control of PWM rectifier with simple calculation," *IEEE Trans. on Power Electronics*, Vol. 28, No. 7, pp. 3428 - 3437, Jul. 2013.
[12] J. Hu and Z. Q. Zhu, "Investigation on switching patterns of direct power control strategies for grid-connected DC - AC converters based on power variation rates," *IEEE Trans. on Power Electronics*, Vol. 26, No. 12, pp. 3582 - 3598, Dec. 2011.
[13] G. Kwon and Y. Suh, "Direct power control scheme of improved command tracking capability for PMSG MV wind turbines," *The Korean Institute of Power Electronics Conference 2015*, pp. 361-362, July. 2015.
[14] B. Wu, Y. Lang, N. Zargari, and S. Kouro, "Power conversion and control of wind energy systems," NJ, *IEEE Press*, 2011, ISBN 978-0-470-59365-3.
[15] M. Malinowski, M. P. Kazmierkowski, and A. M. Trzynadlowski, "A comparative study of control techniques for PWM rectifiers in AC adjustable speed drives," *IEEE Trans. on Power Electronics*, Vol. 18, No. 6, pp. 1390 - 1396, Nov. 2003.
[16] J. Kim, S. Jou, D. Choi, and K. Lee, "Direct power control of three-phase boost rectifiers by using a sliding-mode scheme," *Journal of Power Electronics*, Vol. 13, No. 6, pp. 1000 - 1007, Sep. 2013.
[17] K. Lee, Y. Suh, and Y. Kang, " Loss analysis and comparison of high power semiconductor devices in 5MW PMSG MV wind turbine systems," *Journal of Power Electronics*, Vol. 15, No. 5, pp. 1380 - 1391, Sep. 2015.
[18] T. Kang, T. Kang, B. Chae, K. LEE, and Y. Suh, "Comparison of efficiency for voltage source and current source based converters in 5MW PMSG wind turbine systems," *The Transactions of the Korean Institute of Power Electronics*, Vol. 20, No. 5, pp. 410 - 420, Oct. 2015.

This work was supported by the National Research Foundation of Korea (NRF) grant funded by the Korea government (MSIP) (*No. 2010-0028509*) & (*No. 2014R1A2A1A11053678*).

Gookmin Kwon was born is Jeonju, Korea, in 1989. He received his B.S. in Electrical Engineering from Chonbuk National University, Jeonju, Korea, in 2014, where he is currently working toward his M.S. in Electrical Engineering. His current research interests include the power conversion systems of high power for renewable energy sources and medium voltage electric drive systems.

Yongsug Suh was born in Seoul, Korea. He received his B.S. and M.S. in Electrical Engineering from Yonsei University, Seoul, Korea, in 1991 and 1993, respectively, and his Ph.D. in Electrical Engineering from the University of Wisconsin, Madison, WI, USA, in 2004. From 1993 to 1998, he was an Application Engineer in the Power Semiconductor Division of Samsung Electronics Co. From 2004 to 2008, he was a Senior Engineer in the Power Electronics and Medium Voltage Drives Division of ABB, Turgi, Switzerland. Since 2008, he has been with the Department of Electrical Engineering, Chonbuk National University, Jeonju, Korea, where he is currently an Associate Professor. His current research interests include the power conversion systems of high power for renewable energy sources and medium voltage electric drive systems.